Materials and Design 34 (2012) 501–508

Contents lists available at SciVerse ScienceDirect

Materials and Design

journal homepage: www.elsevier.com/locate/matdes

Formability of lightweight alloys by hot incremental sheet forming

G. Ambrogio *, L. Filice, F. Gagliardi

Dept. of Mechanical Engineering, University of Calabria, 87036 Rende (CS), Italy

ARTICLE INFO

Article history:
Received 14 April 2011
Accepted 15 August 2011
Available online 25 August 2011

Keywords:
A. Non-ferrous metals and alloys
C. Forming
H. Selection for material properties

ABSTRACT

In this paper, the performance of a novel manufacturing process, named hot incremental sheet forming, is investigated; this process is characterized by low cost and time saving. Three lightweight alloys, typically utilized in the aircraft and aerospace industries, were formed by supplying a continuous current in order to generate a local heating. The latter allows a higher formability as compared to cold forming. The workability windows of the materials were drawn confirming the approach suitability and allowing a quick process design when a given geometry is desired. Finally, considerations on the microstructural changes and surface roughness were also supplied. The details are, carefully, explained in the manuscript.

1. Introduction

Traditional manufacturing processes for sheet metal forming industry usually carry high cost and long lead time for short production runs. About 20 years ago, Schmoekel [1] predicted that metal forming equipment would become more flexible by increasing in automation. Accordingly, a new class of processes truly enable flexible production of complex metal parts, either in small batch lots and short lead times [2]. At the same time, the application of lightweight components is another challenge in modern transportation engineering (Fig. 1). Mass reduction is, in fact, necessary due to economical and ecological reasons as well as to improve product properties [3].

Several reasons suggest the use of such materials from an engineering point of view (Fig. 1), in fact, lightweight materials are characterized by a high strength to density ratio. On the other hand, low formability is, usually, typical of this group of materials; consequently, the conventional processes have to be redesigned.

Possible solutions are:

- forming at elevated temperatures, in this case forces reduce and ductility increases since additional slip lines are activated. This alternative results particularly suitable for magnesium alloys;
- superplastic forming, which is characterized by grain size below 10 μm. This method is utilized for aluminum and titanium;
- tixoforming, where material is formed in a semi-solid state.

In this study, incremental sheet forming process (ISF), firstly described in 1994 [4], was considered as an alternative to hot stamping of lightweight alloys. Aircraft bodies and aerospace components are typically composed by lightweight materials such as aluminum, titanium and magnesium alloys.

However, hot stamping implies high cost and setup time. On the contrary, ISF process does not require expensive conventional equipment and long setup operations. At the same time, high achievable strains and flexible manufacturing methods make this process very promising for the applications. ISF was introduced as the natural evolution of spinning process [5]. Up to now, several studies were carried out to show the process suitability and its main characteristics. At the beginning, the studies were focused on the very simple process tooling; Matsubara [4] utilized a NC milling machine to successfully form various sheet metal parts. Iseki and Kumon [6] characterized the forming limit of ISF using a spherical roller.

However, warm and hot forming conditions, which make the process equipment more complex, are necessary to work lightweight alloys. The present study is addressed to propose a solution in this direction by using the ISF.

2. Lightweight alloys for aerospace applications

Lightweight components are of crucial interest for all branches that produce moving masses. Reducing structural weight is one of the most important goals for the improvement of the aircrafts performance. This aim can be obtained by progress in materials. Aluminum alloys have been the most widely used structural materials in aircrafts for several decades; however, new alloys and engineered materials are now emerging. In aircraft applications, lightweight materials characterized by high mechanical properties, i.e. fatigue performance, fracture toughness and strength to density ratio, are

* Corresponding author. Tel.: +39 0984494640; fax: +39 0984494673.
E-mail addresses: g.ambrogio@unical.it (G. Ambrogio), l.filice@unical.it (L. Filice), f.gagliardi@unical.it (F. Gagliardi).
URL: http://tsl.unical.it (G. Ambrogio).

0261-3069/$ - see front matter
doi:10.1016/j.matdes.2011.08.024

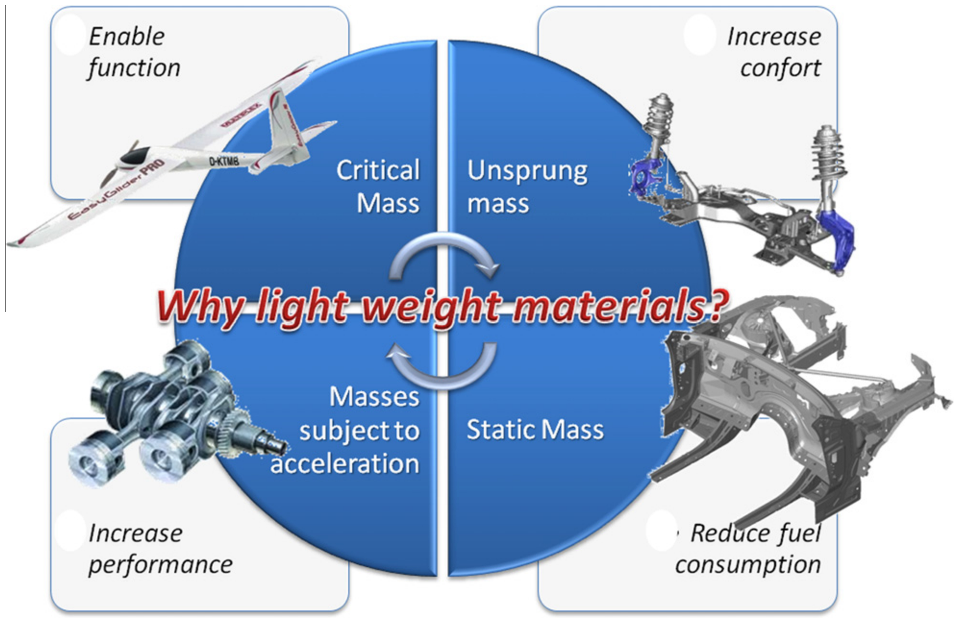

Fig. 1. Purpose of light weight components.

strongly required to reduce both fuel wasting and flight time. In the present study three alloys widely applied in aerospace field were considered: the aluminum alloy AA2024-T3, the magnesium alloy AZ31B-O and the titanium alloy Ti6Al4V.

The AA2024-T3 can be considered as an advanced aluminum alloy for aerospace applications due to its high fatigue performance, high formability, and superplastic behavior to meet the needs for lowest structural weight, highest damage tolerance and durability [7]. Copper, as an alloying element, is used to obtain high strength in AA2024 up to 150 °C [8]. As all the heat treated aluminum alloys, the AA2024-T3 is difficult to weld by fusion techniques, due to the defects in the welding line. However, recent researches have highlighted that the AA2024 can be safely welded by Friction Stir Welding (FSW) [9,10].

The magnesium alloy AZ31B, in the annealed state, is characterized by strength-to-weight ratio lower than AA2024-T3; however, density is equal to 1.77 kg/dm^3, approximately 36% lighter than aluminum. Magnesium provides low ductility for cold forming operations due to its closed packed hexagonal structure at room temperature. Above 225 °C, additional sliding planes are activated increasing ductility and reducing the yield stress [11]. Thus, magnesium alloy ductility and formability is increased by means of heating and mechanisms not active at room temperature [12].

Titanium is another material extensively utilized in the aircraft industry due to the better strength-to-weight ratio compared to steel and aluminum, corrosion resistance and high strength at elevated temperatures. Titanium alloys need to be hot worked for their tendency to strain harden at low temperatures and for their alpha–beta microstructure which is extremely sensitive to temperature (i.e. Ti6Al4V). The hot brake forming is one of the most common manufacturing processes used to fabricate titanium parts made of simple bends [13]. Straight bends (i.e. ribs, stringers, etc.) are titanium parts in aircraft. In the main structure of the Airbus A330/340, titanium only accounts for 7% of the weight, in contrast to the engine where titanium is the main material in terms of volume [3]. In the application of a helicopter rotor head, titanium is used for its highest durability under dynamically changing loads [3,14,15].

However, manufacturing processes need to be optimized or new processes need to be designed to replace stainless steel or other conventional material type by newer lightweight alloys.

According to that, workability of the highlighted alloys was investigated through the design of an innovative and flexible technological process, named hot incremental sheet forming (HISF).

3. Incremental sheet forming of lightweight alloys

In the last years, different works were proposed to analyze the manufacturing of lightweight materials using ISF process. In 2008, Hussain et al. [16] firstly investigated the formability of commercial pure titanium; lubricant, tool pitch, tool feed rate and diameter were changed in the experimental tests. The tests were executed at room temperature; it was found out that the formability, in terms of maximum inclination angle, decreases at increasing the value of all the above parameters. However, formability of industrial titanium alloys is truly low at room temperature. The same consideration can be done for magnesium alloys, such as AZ31B [17].

On the other hand, few works are reported in literature about AA2024 aluminum alloy. In 2010, Hussain et al. [18] investigated the formability of this alloy in ISF process; the annealed and pre-aged conditions were taken into account. A cold forming window was gotten and the influence of the relevant operating parameters was identified. However, it has to be highlighted that cold formability of the heat-treatable AA2024-T3 is low [7]. Concluding, ISF cannot be used to work lightweight alloys for aerospace applications at room temperature. Duflou et al. [19] introduced the hot incremental sheet forming of Ti6Al4V. In such a study, a Nd-YAG laser supplying a power of 500 W was used as heat source; the experimental set-up required a 6-axis robot, equipped with a tool spindle mounted on a strain gauge based force/torque sensor. The results were encouraging, but the proposed technique presents a point of weakness due to the complex and expensive equipment [19].

Fan et al. [20] introduced a cheaper technique based on the use of an electric current to heat the sheet metal. The electric current was supplied by a DC power source while a closed circuit was built through the forming tool and the blank. The maximum drawing angle and the part accuracy were investigated in the paper. In 2010, the Fan et al. [21] used this technique to work the Ti6Al4V alloy demonstrating that the material can be suitably formed by electric hot incremental forming in a range of 500–600 °C with a slight oxidation.

In the work here proposed, electric hot incremental sheet forming is utilized for the manufacturing of different lightweight alloys. The main objective of the work was to identify the working windows as a function of the maximum wall inclination angle and the heat flux required to safely shape the part. Moreover, in order to supply additional information from a qualitative and quantitative point of view both the microstructural and surface roughness analyses were executed.

4. Experimental set-up

According to Fan et al. [20], the experimental tests were carried out by using the equipment depicted in Fig. 2.

A DC power supply was utilized in order to guarantee a suitable voltage (V) at the ends of a closed circuit created by linking the blank and the tooling. A proper feedback control ensured the generation of the desired current level within the range 0–1000 A, ensuring a suitable stability of the material heating. In particular, the low alloy steel frame is always utilized in ISF to clamp the blank along its perimeter. The punch was realized by high speed steel (HSS); in fact, it must have good mechanical resistance at high temperature to avoid its break or excessive wear during material processing.

The electrical connection between cable and punch deserves a specific treatment since the punch rotates during the process: a suitable system was designed and realized by using a graphite slider forced against the rotating tool. The graphite was chosen taking into account its high conductivity and low friction. A groove was machined into the graphite; two springs were used to push the graphite slider against the punch allowing a proper electrical connection; they were placed inside the box (Fig. 3).

The electrical resistance of the whole circuit (R_{total}) is the sum of different resistances provided by each conducting body. The serial resistance of the circuit, without the contact resistance between the punch and the sheet, ($R_{Circuit}$) was estimated using an Ohmmeter before the operations. More in detail, this measure was executed by adding the electrical resistance of two semi-circuits: the first one is the line between the power supply plug and the punch, the second one is the line between the sheet and the other power supply plug. The measures were executed with the rotating tool and they showed a suitable resistance constancy. According to that, taking into account the contact resistance at the interface between the punch and the sheet ($R_{Contact}$), the resistance of the whole circuit (R_{total}) can be assumed as:

$$R_{total} = R_{Circuit} + R_{Contact} \tag{1}$$

Since the $R_{Circuit}$ was known, the $R_{Contact}$ was continuously calculated during the tests as:

$$R_{Contact} = \frac{V}{I} - R_{Circuit} \tag{2}$$

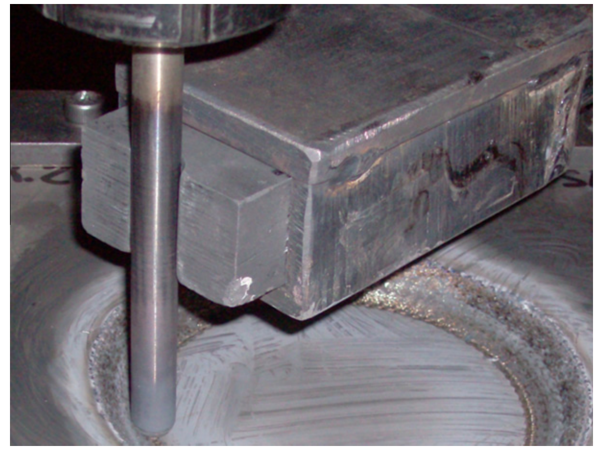

Fig. 3. The designed system to allow the contact between cable and punch.

In Eq. (2), V is the voltage and I the flowing current. $R_{Contact}$ is the highest resistance value in the whole circuit and it is responsible of the highest heat generation by Joule's effect. Joule's first law states that the heat dissipation rate in a resistive conductor is proportional to the square of the flowing current and its resistance.

The generated heat is a key variable because it increases the material temperature and, consequently, its ductility. The closed circuit has to be electrically insulated from the milling machine that is used to carried out the ISF; a wood support was placed at the bottom of the equipment for this purpose.

The sliding area was cooled using a cold air flow.

As above introduced, aluminum AA2024-T3, magnesium AZ31B-O and titanium Ti6Al4V alloys were analyzed. Their main mechanical properties are reported in Table 1. The initial thickness for each material was equal to 1 mm.

The molybdenum disulfide (MoS_2) was used as lubricant in the experiments for each material; it is a solid inorganic compound used to reduce friction between sheet and tool. A thin layer was brushed on the sheet surface before each test.

The punch tip had a diameter equal to 12 mm. A wooden made backing plate was positioned under the sheet allowing a working area equal to 140 mm. In this way, the major base of the shape was positioned really close to the support, thus ensuring the good precision of the final component and the rightness of the formability analysis as conventional recognized [2]. A frustum of cone, which is conventionally recognized as a benchmark shape [2], was produced: the major base and the final depth were fixed to 120 mm and 40 mm, respectively. According to other researchers, a depth of 40 mm guarantees the steady-state conditions by using a 12 mm tool diameter [22]. The experiments were set in order to investigate the critical inclination angle changing the current intensity and, consequently, the heat generated by Joule's effect.

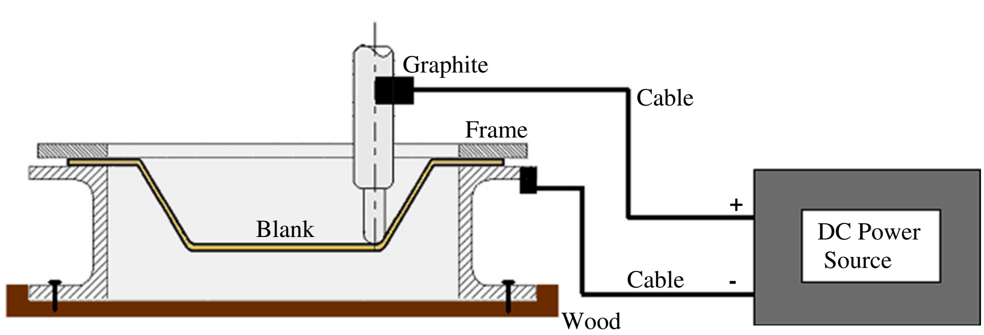

Fig. 2. Sketch of equipment used for hot ISF.

Table 1
Mechanical properties at room temperature for the investigated materials.

	AA2024-T3	AZ31B-O	Ti6Al4V (Grade 5)
Tensile strength-yield (MPa)	350	150	1100
Tensile strength-ultimate (MPa)	475	255	1170
Modulus of elasticity (MPa)	73.1	45	114
Elongation at break	14%	21%	10%
Density (kg/dm^3)	2.78	1.77	4.43

5. Experimental tests

The tool speed rotation (S = 120 rpm.) and the tool depth step (p = 1 mm) were kept constant during all the investigations in order to simplify the analysis.

The aim of the work was the construction of workability windows taking into account the thermal effects due to the Joule's laws, basing only on a phenomenological point of view.

In fact, only the maximum slope angle was considered avoiding any consideration regarding the microstructural material evolution.

For this aim, ISF tests were firstly carried out without material heating in order to find the critical drawing angle at room temperature, identifying the window "starting point". Subsequently, the tests were performed locally heating the sheets.

The process variables are: I (current intensity, A), v (tool feed, mm/s), t (sheet thickness, mm), w (arch of contact, mm) (Fig. 4). Furthermore, $R_{Contact}$ is the contact resistance, which can be considered as a constant after the first coils of the tool trajectory. The specific energy (E_{sp}) was defined to quantify the heat supplied to the material during each test, according to the following ratio:

$$E_{sp} = \frac{R_{Contact} * I^2}{v * t * w} \tag{3}$$

The E_{sp} was varied by changing I and fixing v, t and w; the latter is obtained as:

$$w = \frac{D_p}{2}\alpha \tag{4}$$

being D_p the tool diameter and α the inclination angle (Fig. 4). At the process beginning, the contact between punch and sheet can be represented as a single point; it increases, coil after coil, up to the punch depth becomes equal to its radius. For this reason, the current intensity (I) goes from zero to a regime value supplying a constant E_{sp} during the process.

In this way, the workability window for each material was built by identifying the boundaries between safe and failure regions; starting by the critical angle at room temperature and with increments of 5°, the working areas were individuated as a function of the E_{sp} value.

6. Discussion of the results

First of all, the experimental investigation highlighted the feasibility of the method introduced by Fan et al. [20]: the electrical heating, in fact, resulted cheaper than the solution proposed by Duflou et al. in [19]. Naturally, the addition of a current flow increases the complexity; for this reason, an accurate process control, based on the specific energy E_{sp}, was proposed. This greatness was monitored to avoid part burning that can be a natural consequence of a not optimized manufacture [21].

The experimental investigation was carefully executed taking into account three different aspects:

- first of all, the material formability was observed from a phenomenological point of view, to derive workability windows;
- after that, "*a posteriori*" analysis on the substrates was executed to highlight the influence due to electrical heating from a microstructural point of view;
- finally, the surface roughness was measured to evaluate the product quality and the industrial applicability of the proposed approach.

Each aspect is carefully detailed in the following sections.

6.1. Design of workability windows

A preliminary experimental investigation was carried out to find the formability limit at room temperature for each material. Due to the utilized equipment and the imposed shape profile, wall inclination angles lower than 20° were not considered. The results at room temperature are summarized in Table 2. A "*sound*" component

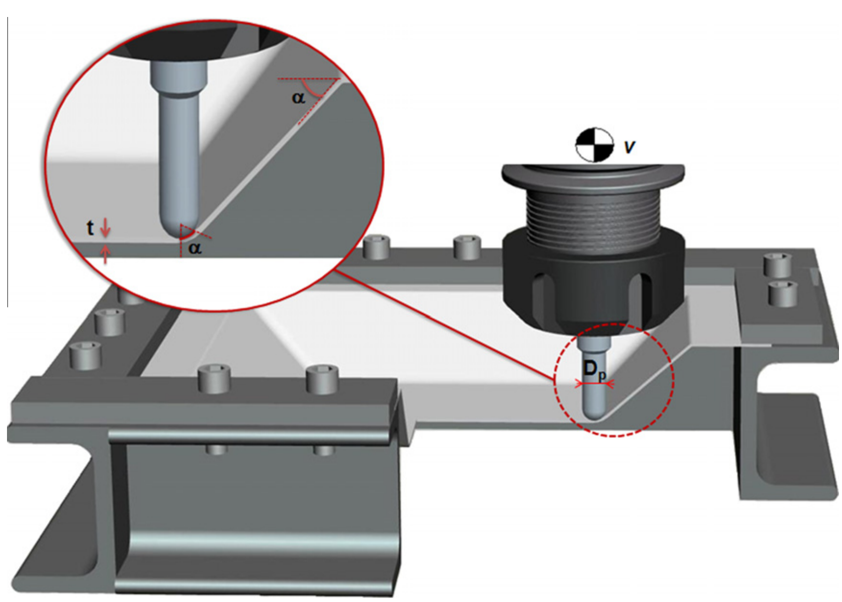

Fig. 4. Detail of the contact area.

Table 2
Experimental results at room temperature.

Wall inclination (°)	AA 2024-T3	AZ31B-O	Ti6Al4V
20	Sound	Broken (h_f = 20 mm)	Sound
25	Sound	Broken (h_f = 6.5 mm)	Broken (h_f = 20 mm)
30	Sound	Broken (h_f = 3 mm)	Broken (h_f = 18 mm)
35	Broken (h_f = 13 mm)		Broken (h_f = 15 mm)
40	Broken (h_f = 11 mm)		

means that the final height of 40 mm was reached; otherwise, the final height (h_f) measured during the failed tests is reported.

As expected, the magnesium AZ31B-O presents the worst behavior at room temperature, due to the closed packed hexagonal structure. On the contrary, the aluminum AA2024-T3 can be safely formed up to a wall inclination angle of 30°. Finally, the formability limit of titanium Ti6Al4V at room temperature is 20 °C.

After this preliminary investigation, the experiments were performed locally heating the sheet. As expected, adding an heat flux to the material its formability increases. The maximum reached wall inclination angle was 40° for AA2024-T3, 60° for AZ31B-O and 45° for titanium Ti6Al4V. The components with the highest wall inclination angle are shown in Fig. 5. The cold analysis confirms the knowledge traceable from literature review [16–18], while some differences were observed during the hot-forming of Ti6Al4V [21].

According to the already explained strategy, for each material the workability window were built (Figs. 6–8).

The same conclusions can be derived for all the analyzed materials:

– the grey band represents the transition zone from unsafe to safe condition;
– sound components cannot be obtained if energy values are below the unsafe curve;
– energy values which are higher than the burned boundary lead to the sheet burning;
– the workability area, for each material, is delimited by the safe curve and burned boundary one.

According to the expected results, supplied energy has to be a trade-off between material heating and its damaging. The burned boundary individuates the energy level which generates a great material oxidation, especially in the sheet bottom side. Punch action, in fact, tends to destroy the oxide layer during its formation. Furthermore, the material melts down increasing the supplied energy.

Finally, with respect to the state of the art [18,20,21], the study here addressed supplied a design tool which facilitates the process control; in fact, the workability windows have to be regarded as design charts able to help the process analyst to individuate the optimal energy level to obtain a given inclination angle. Of course, within the admissible range, the optimal value is close to the safe curve in order to reduce as possible the temperature and, as a consequence, the thermal effects on the processed material.

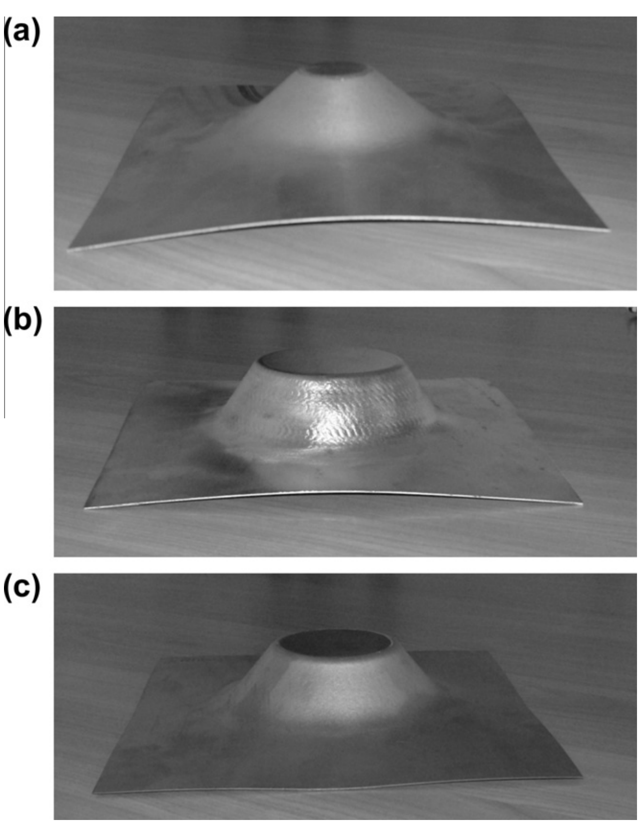

Fig. 5. Experimental results for (a) AA2024-T3, (b) AZ31B-O, and (c) Ti6Al4V.

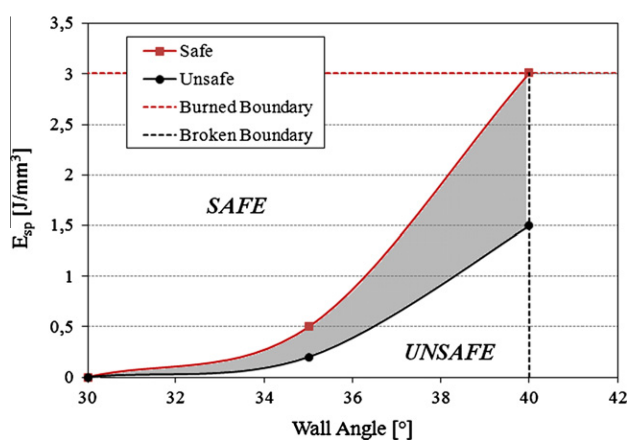

Fig. 6. Workability window for hot incremental sheet forming of AA2024-T3.

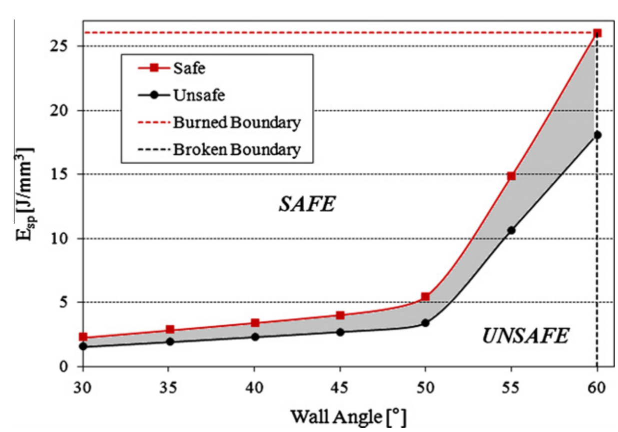

Fig. 7. Workability window for hot incremental sheet forming of AZ31B-O.

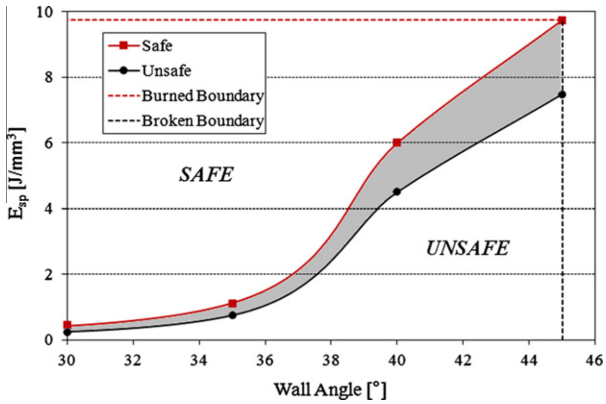

Fig. 8. Workability window for hot incremental sheet forming of Ti6Al4V.

6.2. Analysis of material substrates

A preliminary analysis of the temperature effect on the materials was carried out taking into account their morphology; the latter was qualitatively analyzed by means of Scanning Electron Microscopy (SEM). Fig. 9 shows the SEM images of the investigated substrates, with and without electrical heating; for sake of shortness, the substrates of sound components obtained by maximum current value were reported.

The specimens have been obtained causing a brittle cracking along the section, after a quick material cooling in liquid nitrogen. In this way, the surface profile is directly related to the grains structure of both the "as received" and "electrically heated" material.

The following conclusions for each material can be derived:

- as expected [7], the original AA2024-T3 substrate presents high density which decreases after the test due to the current addition. More in detail, the substrate becomes more porous and worse organized; in fact, lamellar plans, randomly oriented, are evident after forming by heating the sheet with 100 A;
- as concern the AZ31 substrate, lamellar plans are partially visible at the beginning. The current addition clearly introduces more evident and well organized structure; in particular, a dense lamellar structure can be easily recognized by the micrograph obtained by forming the specimens supplying a current of 260 A;
- as known [23], the original structure is well organized: the porosity is evident and the grain distribution appears uniform. By electrically heating, after forming the substrate results less organized; more in detail, the pore size decreases by increasing material temperature. According to that, the final structure of the worked Ti6Al4V results with a higher density (recrystallization).

Although the above observations do not separate the contributions of strain induced and thermal induced recrystallization, they

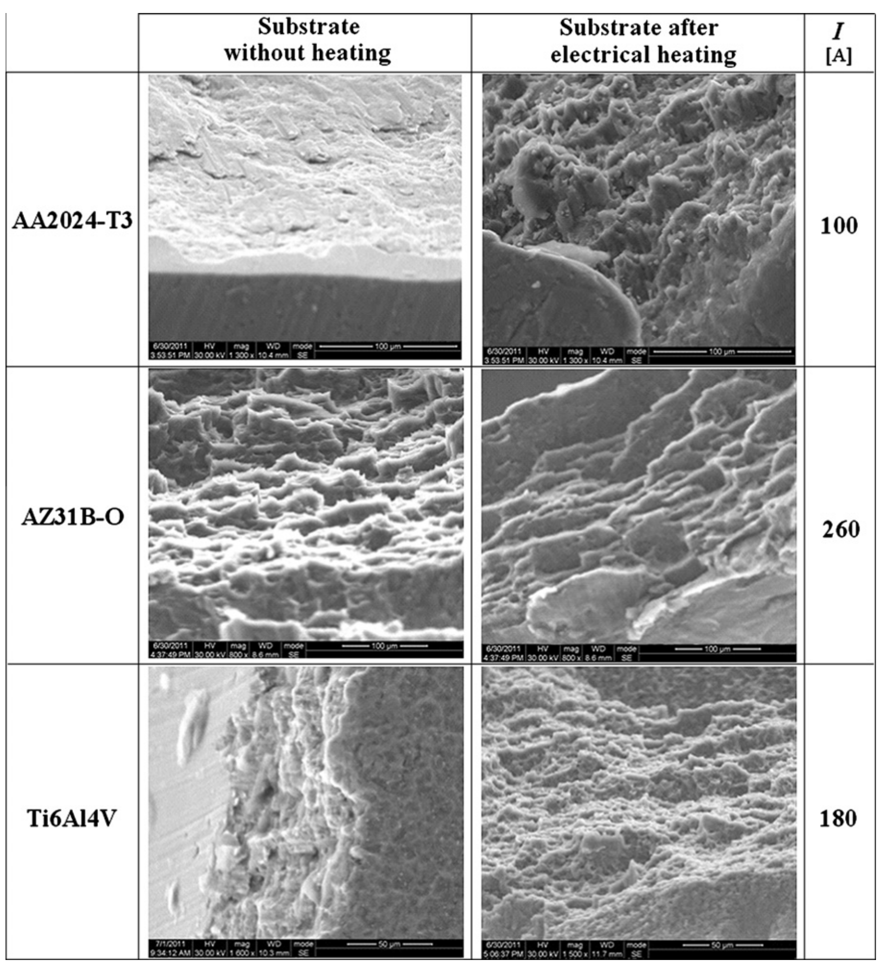

Fig. 9. Micrographs of the internal substrates for the three alloys.

give a clear representation of the substrate configuration after processing.

6.3. Analysis of the surface roughness

Surface quality is an important variable to be taken into account in the global process evaluation; in particular, it represents a weak point in ISF [2]. In this study, the current addition introduces further complexity in the phenomenon evolution; however, if the process is properly executed, the measured surface quality can be compared with the cold manufacture [24].

In the analysis here addressed, the attention was focused on the influence of both the slope angle and the forming energy on the surface roughness. The measurements were carried out by a roughness device and were repeated in five equally spaced zones for each sound specimen. Three parameters were taken into account, i.e. the average roughness height (R_a), the max peak-to-valley height in any one cutoff length (R_{max}) and the average peak-to-valley roughness height (R_z); their average value and standard deviation were reported.

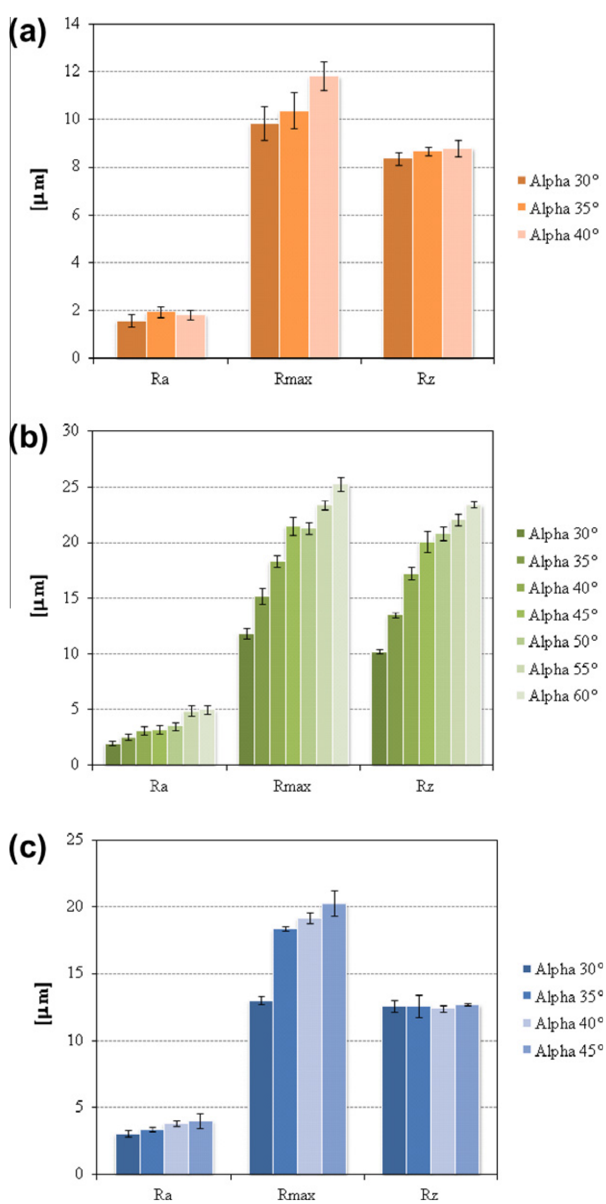

Fig. 10. The roughness measurements for (a) AA2024-T3, (b) AZ31B-O, and (c) Ti6Al4V.

The results highlight a surface quality worsening when increasing the slope angle for each material (Fig. 10); the reasons of this phenomenon are:

(1) the supplied E_{sp} increases if a higher slope angle has to be formed. By this way, material oxidation increases;
(2) the contact zone between punch and sheet increases if higher slope angle has to be reached (Fig. 4). For this reason, each sheet zone is more effected by the punch movement; as consequence, greater damage on the surface quality is caused.

In other words, E_{sp} produces a thermal effect that increases oxidization while the punch pressure influences the mechanical action on the sheet. The punch action is beneficial in terms of oxide layer destroying but reduces the surface quality.

Moreover, significant quality differences between the two sheet sides were observed (Fig. 11).

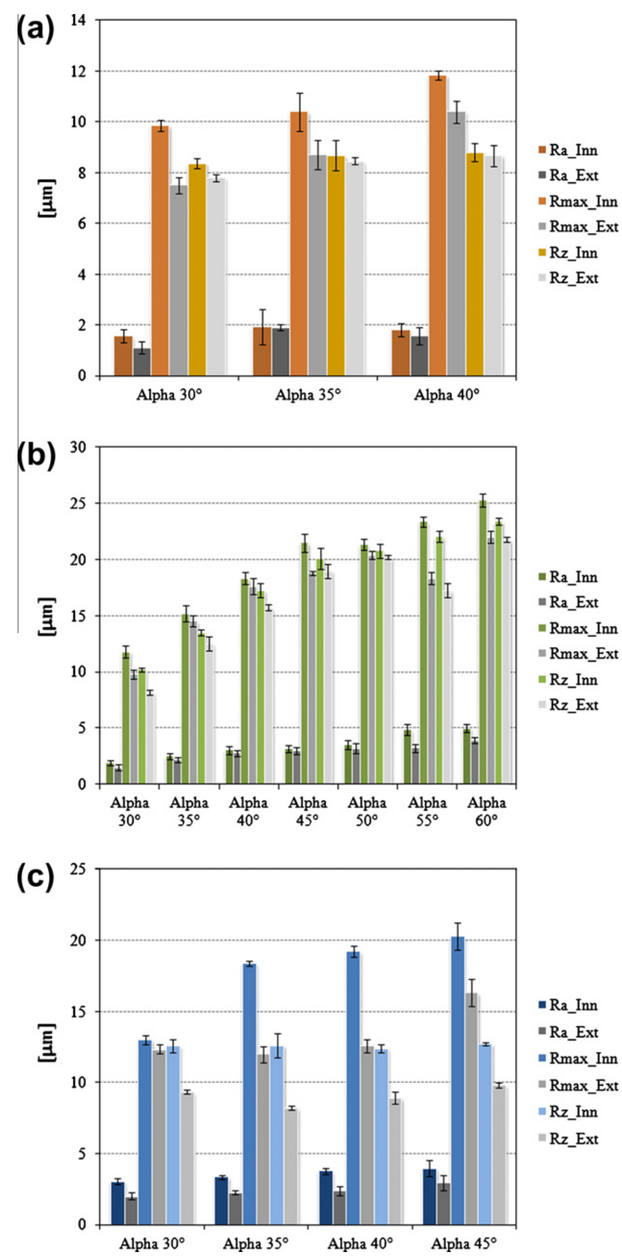

Fig. 11. Difference between internal and external roughness values for (a) AA2024-T3, (b) AZ31B-O, and (c) Ti6Al4V.

The quality of the bottom surface is always better as compared to the one in contact with the punch.

This is due to both the lower temperature reached on the bottom side that reduces oxidation phenomenon and the absence of mechanical actions on the sheet. Anyway, because of the low sheet thickness, the thermal gradient is very low and this reduces the differences between the two sheet sides.

In the industrial applications of lightweight alloys several times just one side of the component needs specific surface characteristics. If the target profile is the one not in contact with the punch, better surface characteristics are shown (Fig. 11).

7. Conclusion

Lightweight alloys represent key materials for the future of manufacturing industry and their use in the aerospace field is a constant topic for researchers of all over the world [7,25]. However, their use is limited by the need of non-room temperature which requires specific equipments and extra-costs for the tool heating. In this study, a simple and effective system based on the Joule's effect was proposed. The incremental forming workability windows were drawn for each investigated material plotting the allowable inclination angle as function of the supplied heating energy; these maps can be used by the process analysts as a suitable tool to optimally design the process when a given inclination angle has to be considered in manufacturing of lightweight components. As concern the microstructural aspects, the results showed a different grain distribution due to both the electrical heating and induced strain, directly dependent on the material properties.

Finally, the surface roughness is influenced by the process characteristics: in fact, the surface quality get worse by increasing the wall slope angle and, as consequence, the supplied energy.

References

[1] Schmoekel D. Developments in automation, flexibilization and control of forming machinery. Cirp Ann-Manuf Technol 1992;40(2):615–9.
[2] Jeswiet J, Micari F, Hirt G, Bramley A, Duflou J, Allwood J. Asymmetric single point incremental forming of sheet metal. Cirp Ann-Manuf Technol 2005;54(2):623–60.
[3] Kleiner M, Geiger M, Klaus A. Manufacturing of lightweight components by metal forming. Cirp Ann-Manuf Technol 2003;52(2):521–43.
[4] Matsubara S. Incremental backward bulge forming of a sheet metal with a hemispherical head tool. J Jpn Soc Tech Plasticity 1994;35:1311–6.
[5] Kalpakcioglu S. A study of shear – spinnability of metals. J Eng Ind-T Asme 1961;83:485–95.
[6] Iseki H, Kumon H. Forming limit of incremental sheet metal stretch forming using spherical rollers. J Jpn Soc Tech Plasticity 1994;35:1336–41.
[7] Huda Z, Iskandar Taibb N, Zahariniea T. Characterization of 2024-T3: an aerospace aluminum alloy. Mater Chem Phys 2009;113:515–7.
[8] Sorrentino L, Carrino L. 2024 aluminium alloy wettability and superficial cleaning improvement by air cold plasma treatment. J Mater Process Tech 2009;209:1400–9.
[9] Thomas WM, Nicholas ED. Friction stir welding for the transportation industries. Mater Des 1997;18(4/6):269–73.
[10] Aydin H, Bayram A, Uguz A, Sertan Akay K. Tensile properties of friction stir welded joints of 2024 aluminum alloys in different heat-treated-state. Mater Des 2009;30:2211–21.
[11] Nghiep Nguyen B, Bapanapalli SK. Forming analysis of AZ31 magnesium alloy sheets by means of a multistep inverse approach. Mater Des 2009;30:992–9.
[12] Palumbo G, Sorgente D, Tricarico L. Tangential bending and stretching of thin magnesium alloy sheets in warm conditions. Mater Des 2009;30:653–60.
[13] Walczyk DF, Vittal S. Bending of titanium sheet using laser forming. J Manuf Proc 2000;2(/4):258–69.
[14] Vanderhasten M, Rabet L, Verlinden B. Ti–6Al–4V: Deformation map and modelisation of tensile behavior. Mater Des 2008;29:1090–8.
[15] Djavanroodi F, Derogar A. Experimental and numerical evaluation of forming limit diagram for Ti6Al4V titanium and Al6061–T6 aluminum alloys sheets. Mater Des 2010;31:4866–75.
[16] Hussain G, Gao L, Zhang Y. Formability evaluation of pure titanium sheet in the cold incremental forming process. Int J Adv Manuf Technol 2008;37:920–6.
[17] Ambrogio G, Filice L, Manco GL. Warm Incremental forming of magnesium alloy AZ31. Cirp Ann-Manuf Technol 2008;57:257–61.
[18] Hussain G, Gao L, Hayat N, Dar U. The formability of annealed and pre-aged AA-2024 sheets in single-point incremental forming. Int J Adv Manuf Technol 2010;46:543–9.
[19] Duflou JR, Callebaut B, Verbert J, De Baerdemaeker H. Laser assisted incremental forming: formability and accuracy improvement. Cirp Ann-Manuf Technol 2007;56(1):273–6.
[20] Fan G, Gao L, Hussain G, Wu Z. Electric hot incremental forming: a novel technique. Int J Mach Tool Manuf 2008;48:1688–92.
[21] Fan G, Sun F, Meng X, Gao L, Tong G. Electric hot incremental forming of Ti–6Al–4V titanium sheet. Int J Adv Manuf Technol 2010;49:941–7.
[22] Filice L, Ambrogio G, Micari F. On-line control of single point incremental forming operations through punch force monitoring. Cirp Ann-Manuf Technol 2006;55(1):245–8.
[23] Donachie MJ. Titanium: a technical guide. Materials Park, OH (USA): ASM International; 2000.
[24] Hagan E, Jeswiet J. Analysis of surface roughness for parts formed by computer numerical controlled incremental forming. J Eng Manuf (Part B) 2004;218:1307–12.
[25] Vermeulen B, van Tooren MJL. Design case study for a comparative performance analysis of aerospace materials. Mater Des 2006;27:10–20.